

### III. A stochastic two-stage reaction model for heavy-ion collisions

Z. Sosin<sup>a</sup>

M. Smoluchowski Institute of Physics, Jagellonian University, Reymonta 4, 30-059 Cracow, Poland

Received: 12 March 2001 / Revised version: 18 May 2001

Communicated by D. Guereau

**Abstract.** We propose a two-stage, stochastic model of heavy-ion reactions. Nucleons becoming participants by mean-field effects or by nucleon-nucleon interactions are transferred to definite final states, creating a PLF, a TLF, clusters, or escaping to continuum. Nucleon transfer probabilities are governed by state densities. In this way different hot particle sources are created which afterwards decay by particle emission.

**PACS.** 24.10.-i Nuclear-reaction models and methods – 25.70.-z Low and intermediate energy heavy-ion reactions – 25.70.Lm Strongly damped collisions – 25.70.Pq Multifragment emission and correlations

#### 1 Introduction

The heavy-ion reaction picture is not a simple one, especially at higher collision energies where the multiplicity of emitted particles increases strongly. At low energies, one observes the emission of light particles plus an evaporation residue or a pair of fission fragments. With increasing energy, the ejectile yield gradually turns into a mixture of light particles and intermediate mass fragments (IMFs,  $Z > 2$ ), and finally is uniquely composed of light particles (see [1,2] and references cited therein).

The reaction mechanism also varies considerably with increasing collision energy. At lower energies, one encounters peripheral or deep inelastic collisions for larger impact parameters, and incomplete fusion (or fusion-fission) for more central collisions. At higher energies, in addition to the projectile-like fragment (PLF) and the target-like fragment (TLF), an intermediate velocity source (IVS) appears, located between the PLF and the TLF. At sufficiently high energies this IVS absorbs most of the dissipated energy, while the PLF and the TLF turn into spectators. In central collisions at sufficiently high energies heavy ions turn into a gas of light particles in a process called vaporization.

In each of these phenomena, nucleons change their initial attachment and energy is dissipated. Energy dissipation is expected to be rather one body for lower energies, because of Pauli blocking, but should become two body at higher energies, when Pauli blocking is less effective. Near the Fermi energy, both energy dissipation scenarios can be expected to compete.

In order to test our understanding of the heavy-ion reaction mechanism in this energy range, experimental results are compared to predictions derived from various

models. One approach uses semi-classical dynamic calculations performed on the microscopic level, *e.g.* BUU [3], VUU [4], BNV [5], LV [6], molecular dynamics calculations [7], fermionic molecular dynamics (FMD) [8], antisymmetrized molecular dynamics (AMD) [9], etc. Such calculations are rather time consuming, however, and not always successful in providing a detailed description of experimental data. Consequently, these methods are frequently replaced by simpler models, which are quite satisfactory in reproducing results of various measurements related to damped collisions and explaining details of the reaction scenario. This will be the approach adopted in the present paper.

The model proposed here belongs to a family of models that includes, for example, those of Harvey [10] and Cole [11], Tassan-Got and Stéphan [12], Durand [13], and Sosin *et al.* [14], based on the Randrup assumption [15] that for higher collision energies, energy dissipation proceeds mainly through stochastic transfer of nucleons between colliding ions. The presented model is an extension of those proposed by Cole [11] and by Sosin *et al.* [14].

In Cole's model [11], the outcome of a peripheral nucleus-nucleus collision is considered to be the result of a random walk in the projectile mass. The number of "steps" is obtained from the Poisson distribution around the average number of NN collisions calculated within the optical limit of Glauber's theory. The NN collisions take place along a trajectory describing the relative motion of projectile and target. The PLF deflection is produced in part by the potential acting between colliding ions, and in part by the recoil effects caused by mass exchange. The Cole model predicts the mass distribution and also the angular distribution of the PLFs. As for the energy spectra, only the mean energy of a fragment is calculated, as a function of the laboratory angle.

---

<sup>a</sup> e-mail: ufsosin@cyf-kr.edu.pl

In an extension proposed by Sosin *et al.* [14] a random walk in the three dimensions of the momentum transfer has also been included, in addition to the random walk in the projectile mass. The de-excitation of the hot PLF and TLF is described by binary decay. In this version of the model it is possible to calculate in a self-consistent manner both the energy and the angular distributions of emitted particles, given as functions of probabilities  $P^+$  and  $P^-$ , that in an elementary interaction the projectile gains or loses a nucleon.  $P^+$  and  $P^-$ , treated as free parameters, have generally been expected to be dependent upon the collision impact parameter (entrance channel angular momentum).

## 2 Description of the model

The model (and its computer realization: the PIRAT Monte Carlo code) presented in this paper treats the heavy-ion collision as a chain of steps. The final result of this chain of steps is governed, on the average, by the maximum value of the thermodynamic probability (entropy), but fluctuations characteristic of the stochastic process are also taken into account. The thermodynamic probabilities are related here to the distribution of the density of states of different subsystems taking part in the collision. Using this model, one can describe the creation and decay of different hot sources of particles, such as the PLF, the TLF and the IVS. The model allows for competition between the mean-field effects and the NN interactions in the overlap zone of colliding nuclei.

In the model a two-stage reaction scenario is assumed:

- i) In the first stage, a number of nucleons becomes reaction participants as a result of mean-field effects and/or two-nucleon (NN) interactions. The participating nucleons are virtually free.
- ii) In the second stage, participating nucleons are transferred to definite states, creating finally a PLF, a TLF, or clusters. They can also escape into continuum. In the PIRAT code this process is treated as a chain of steps.

### 2.1 First stage: mean-field mechanism

In the mean-field mechanism one of the nucleons of the projectile nucleus (P) or target nucleus (T) becomes a participant when runs across a potential window which opens in the region between the colliding heavy ions. The degree and duration of opening depends on the proximity and relative velocity of the heavy ions on their classical Coulomb trajectories. By using parabolic approximation (see, *e.g.*, Tassan-Got and Stéphan [12]) one obtains the values of the potential barrier transmission probability across the window. For a given heavy-ion impact parameter,  $b_{\text{HI}}$ , the average number of nucleons crossing the potential window  $\langle n_{\text{cr}} \rangle$  is calculated. The P and T nucleons are treated as a Fermi gas. For each  $b_{\text{HI}}$ , the number of participating nucleons is obtained by a Monte Carlo procedure from the Poisson distribution around  $\langle n_{\text{cr}} \rangle$ .

### 2.2 First stage: two-nucleon mechanism

In the NN mechanism two nucleons, one from the P and the second from the T, collide in the overlap zone of the P and T nuclei, where for larger collision energies and/or larger collision parameters the Pauli principle becomes less restrictive. The nucleons of such a pair become reaction participants. The probability of a NN collision depends on the NN interaction cross-section, the convolution of the P and T densities in the overlap region, and the available momentum space.

For a given  $b_{\text{HI}}$  and with no Pauli blocking, the average number of NN collisions per event,  $\langle n_{ij}(b_{\text{HI}}) \rangle$ , is calculated in the modified optical limit of the Glauber theory, along the heavy-ion trajectory in the entrance channel potential. Here,  $i, j$  denotes n (neutron) or p (proton), respectively.

$$\langle n_{ij}(b_{\text{HI}}) \rangle = (I_i I_j) / (A_P A_T) \int dt v(t) \times \int d^3 \mathbf{r} \sigma_{ij}(E(t)) \rho_P(\mathbf{r} - \mathbf{r}_P(t, b_{\text{HI}})) \rho_T(\mathbf{r} - \mathbf{r}_T(t, b_{\text{HI}})), \quad (1)$$

where  $\mathbf{r}_P(t, b_{\text{HI}})$ ,  $\mathbf{r}_T(t, b_{\text{HI}})$  define the CM positions of the colliding ions, and  $\rho_P$ ,  $\rho_T$  the corresponding matter density distributions. The NN interaction cross-section,  $\sigma_{ij}$ , depends on the colliding pair  $i, j$  and on the average relative NN energy,  $E(t)$ . This energy is a function of the average nucleon energies inside the P and T nuclei and of the relative P-T energy, which depends on the P-T distance. The relative P-T velocity,  $v(t)$ , ( $t$  denotes time) is calculated from the entrance channel interaction potential. The scaling factor in (1) depends on the projectile and target nucleus mass numbers  $A_P$ ,  $A_T$  and on the number  $I_i$  or  $I_j$ , of “ $i$ ” or “ $j$ ” nucleons in the P or T nucleus, respectively.

When the interaction of heavy ions is neglected one obtains straight lines instead of the entrance channel heavy-ion trajectories (as in the original Glauber theory) and a result different from (1) (see Karol [16]).

In order to calculate the distribution of  $n_{ij}$  and to take into account the Pauli blocking effect, the following procedure is applied. The nucleons inside heavy ions are treated as a Fermi gas with the Fermi momentum proportional to  $\rho^{1/3}$ . Each nucleon obtains initial position and momentum in a Monte Carlo procedure taking into account the P and T matter density distributions.

The distribution of  $n_{ij}$  is given by the NN collision probability  $P_{ij}$ , calculated for all pairs of nucleons, and for the Pauli blocking effect checked each time.

$$P_{ij} = C(b_{\text{HI}}) \exp \left[ - (b_{\text{NN}} / 2^{1/2} \sigma)^2 \right] (1 - P_B). \quad (2)$$

Here  $b_{\text{NN}}$  is the NN collision parameter and  $\sigma = K \sigma_0$ . This Gaussian (2) has a half-width,  $2.35\sigma$ , of two fermi (about  $2R_N$ , where  $R_N$  is the nucleon radius) multiplied by  $K$ , a factor taking into account the isospin dependence of  $\sigma_{\text{NN}}$ .  $K^2 = \sigma_{ij} / \sigma_{\text{np}}$ . The Pauli blocking factor  $(1 - P_B)$  is equal to unity when after a NN collision the nucleons find free places in the momentum space. Otherwise,  $(1 - P_B) = 0$ . Isotropy is assumed in the post-collision velocity distributions of the NN pairs. The value of the normalizing

factor  $C(b_{\text{HI}})$  is obtained from a condition, that for  $(1 - P_{\text{B}}) = 1$ , the average number of NN collisions per event,  $\langle n_{\text{NN}} \rangle$ , calculated from (2) should be the same as for (1).

### 2.3 Second stage: nucleon transfer

In the second stage, participating nucleons are transferred to different objects of the system consisting of the projectile remnant (PR), the target remnant (TR), clusters and other participating nucleons. Creation of clusters begins from the coalescence of two participating nucleons. Each transfer changes the state of the system. The transition probability may be calculated from the Fermi rule:  $P_{ik} = (2\pi/\hbar)|T_{ik}|^2\rho_k$ . It is argued (see, *e.g.*, Gross [17]) that the final density of states,  $\rho_k$ , is usually the dominant factor and the square of the  $T$  matrix is roughly constant.

Similarly as in the micro-canonical approach (see, *e.g.*, Gross [17]) we assume that all permitted micro-states are equally probable. In the Gross model, the permitted micro-states have to obey the conservation laws of the total energy, momentum, and angular momentum, baryon and charge numbers. In our model, the accessible phase space is additionally limited by the constrains: i) the existing projectile and target remnants may only absorb particles; ii) the PR, TR, and cluster momenta and angular momenta are determined by the nucleon transfer process.

The PIRAT code probes the accessible phase space in the following way. The nucleon transfer is treated as a stochastic process with the number of steps equal to the number of participating nucleons,  $n$ . The participating nucleons obtain their label numbers randomly, from 1 to  $n$ . The same numbers are used to label the consecutive steps of the stochastic process chain.

The final result of a heavy-ion collision depends on the options chosen in each step by participating nucleons. The possibilities include:

- re-creation of the bond with the mother nucleus;
- creation of a bond with the other nucleus, another participating nucleon, or a cluster of participating nucleons produced in an earlier step.

In step  $k$ , a nucleon with the label  $k$  may join the TR or the PR or a nucleon with a  $k' > k$  label. All the  $k' < k$  nucleons have been taken into account in the earlier steps of the process chain. Alternatively, nucleon  $k$  may remain free and join the group of particles of intermediate velocity. In fact, nucleon  $k$  could be joined in the earlier steps by a certain number of participating nucleons. In such case it is cluster  $k$ , rather than participating nucleon  $k$ , which exercises the different options possible for step  $k$ . This coalescence process leads to the formation of larger clusters in the gas of participating nucleons. At the end of the stochastic process (chain of steps) one gets the PLF, the TLF and the remainder of the gas of participating nucleons will form the intermediate velocity source, IVS.

After each reaction step, four regions of the phase space are accessible for participating nucleons:

- 1) the TR phase space;
- 2) the PR phase space;

3) the phase space of the participating nucleons that are treated as an excited nucleon fermion gas (NFG);

4) the phase space of clusters (CL) created in the earlier steps.

A participating nucleon (cluster) in step  $k$  may exercise one of  $j$  different options ( $1 < j < (n - k + 2)$ ) corresponding to phase spaces (1) to (4), each with a thermodynamic probability  $\Omega(k, j)$ . In order to obtain the  $\Omega(k, j)$  values, the PIRAT code computes the density of states for each object which is present at step  $k$ .

For internal degrees of freedom, the density of states of the TR, PR, CL and NFG objects (after joining a participating nucleon) is calculated as for a Fermi gas:

$$\Delta\Omega_i = \frac{(2s_i + 1)\pi^{1/2}}{12a_i^{1/4}E_i^{5/4}} \exp\left[2(a_i E_i)^{1/2}\right], \quad (3)$$

where  $i$  denotes TR, PR, CL or NFG, respectively,  $s_i$  is the fragment spin and  $E_i$  is the thermal component of its excitation energy. The density of states parameter  $a_i = A_i/\varepsilon_i$ . Here  $A_i$  is the mass of the subsystem, and  $\varepsilon_i$  denotes a parameter which in general depends on  $A_i$  and  $E_i$  (see Bonche *et al.* [18]). Equation (3) is used for fragments with  $A > 3$ . Fragments with  $A < 4$  are treated as cold ones, similarly as in the Bondorf paper [19].

The excitation energy  $E_i$  has to be calculated for each step  $k$  and option  $j$  of the chain of steps. For each  $(k, j)$  the TR, PR, CL and NFG objects have certain ground-state energies and momenta (kinetic energies), and interact with each other via certain potentials. For the TR-PR interaction it is the Coulomb plus proximity potential, and for all other  $(i, j)$  pairs a potential defined as:

$$\begin{aligned} V_{ij}(r) &= (Z_i Z_j / r) & \text{for } r \geq R_{\text{int}}, \\ V_{ij}(r) &= (Z_i Z_j / R_{\text{int}}) & \text{for } r < R_{\text{int}}, \\ R_{\text{int}} &= r_{\text{int}}(A_i^{1/3} + A_j^{1/3}). \end{aligned} \quad (4)$$

In the clusterization process, the clusters thus created may sometimes overlap. It is assumed that they begin to interact when their mutual distance is larger than  $R_{\text{int}}$ . Their separation is insured by the fact that clusters are born with individual velocities.

Summation of the ground state and kinetic energies of fragments with their interaction potentials provides a value of the total energy corresponding to the internal degrees of freedom (excitation energy) of the system. After subtracting the total excitation energy of the step  $k - 1$  one gains the reaction  $Q$  value,  $Q(k, j)$ . The total energy of the system is conserved along the chain but excitation energies of particular subsystems vary according to the  $Q(k, j)$  value. The  $Q(k, j)$  energy is divided among all the involved subsystems having masses  $A > 4$ , with a probability proportional to the corresponding densities of states.

In order to obtain the  $\Omega(k, j)$  values one must include not only the internal degrees of freedom but also those degrees of freedom corresponding to the translational motion. For the system of clusters and nucleons which already left the NFG system, the translational motion density of

states,  $\Delta\Omega_{N,CL}^{tr}$ , may be calculated from the entropy  $S^{tr}$ :

$$\Delta\Omega_{N,CL}^{tr} = \exp S^{tr}, \quad (5)$$

and

$$S^{tr} = - [\partial F^{tr} / \partial T]_{V, N_i}, \quad (6)$$

where  $F^{tr}$  is the free energy of translational motion and  $T$ ,  $V$ , and  $N_i$  denote respectively temperature, volume, and number of different particles of the system. Free energy  $F^{tr}$  is given as (see, *e.g.*, [18]):

$$F^{tr} = -T \sum_{(A,Z)} \{N_{A,Z} \ln [g_{A,Z} (V/\lambda_T^3)] A_0^{3/2}\} \\ + T \ln [(V/\lambda_T^3) A_0^{3/2}]. \quad (7)$$

Here  $A$ ,  $Z$  denotes the cluster (nucleon) mass and charge number, respectively,  $A_0$  is the total mass number of the multi-component gas, (N) + (CL),  $g_{A,Z}$  is the degeneracy factor of the ground state of a fragment ( $A < 5$ ) and  $\lambda_T$  is the nucleon thermal wavelength. The  $g_{A,Z} = 1$  value is assumed for  $A > 3$ . The  $T$  value is obtained from the chaotic thermal component of the kinetic energy and the corresponding number of degrees of freedom

$$\lambda_T = (2\pi\hbar^2/m_N T)^{1/2}, \quad (8)$$

and  $m_N$  is the nucleon mass.

For PR and TR, the density of states corresponding to relative motion,  $\Delta\Omega_{PR,TR}^{tr}$ , is assumed to be proportional to the PR-TR relative momentum and to their reduced mass.

The thermodynamic probability  $\Omega(k, j)$  is given now by:

$$\Omega(k, j) = \Delta\Omega_{PR}(k, j) \times \Delta\Omega_{TR}(k, j) \\ \times \Delta\Omega_{NFG}(k, j) \times \prod_{(\text{all CL})} [\Delta\Omega_{CL}(k, j)] \\ \times \Delta\Omega_{CL,N}^{tr}(k, j) \times \Delta\Omega_{PR,TR}^{tr}(k, j). \quad (9)$$

Dividing  $\Omega(k, j)$  by

$$\Omega(k) = \sum_{\text{all } j} \Omega(k, j), \quad (10)$$

one obtains a set of normalized probabilities  $P(k, j)$ . The random number generator now selects one particular option  $(k, j)$  chosen by the participating nucleon (or cluster)  $k$  with the probability  $P(k, j)$ .

After applying the same procedure to each participating nucleon (cluster)  $k$ , one obtains the final path along the chain of steps. Thus, the final result of this chain of steps is governed, on the average, by the maximum value of the thermodynamic probability, but fluctuations are also taken into account.

After formation of all the fragments the PLF and TLF may fuse. This happens when, due to the dissipation of energy and relative angular momentum, a ‘‘pocket’’ appears in the PLF-TLF interaction potential and the energy of the system is smaller than the potential barrier.

## 2.4 Angular momenta and spins

The angular momenta and spins, of the final reaction products are calculated from the initial P (or PR) and T (or TR) angular momenta, and from the angular momenta of the participating nucleons involved. For the P and T spins, the model assumes zero values. In order to calculate the angular momenta of the participating nucleons we assume that their momenta are distributed as in a Fermi gas, and that the initial locations depend upon the mean field and the NN interaction mechanism.

It is assumed that the participating nucleon  $k$  may join a PR, a TR, or a cluster under two conditions:

i) The spin of the final system (nucleus or cluster) is smaller than the maximum spin permitted for that system, since otherwise nucleon transfer is impossible. The value of the maximum spin is taken from one of the GEMINI subroutines [20], extrapolated to the region  $Z < 10$ .

ii) The captured nucleon’s relative angular momentum is smaller than a specified critical value  $L_{cr}$ , where  $L_{cr} = \beta R_{nucl} p_F$ . Here  $R_{nucl}$  and  $p_F$  denote the P (or PR) or T (or TR) radius and Fermi momentum, respectively.  $\beta$  is a coefficient with a value of the order of unity. This condition determines the value of the maximum momentum of a nucleon which can be captured by a nucleus.

## 2.5 Decay of excited fragments and Coulomb trajectories

The decay of the excited fragments is simulated in the code using the GEMINI [20] or alternatively the SIMON [21] subroutine. Charged fragments produced according to the above reaction scenario have individual initial velocities, and are accelerated in the mutual Coulomb field along proper trajectories which are integrated numerically [22].

## 3 Some numerical results

Competition between the mean-field process and the NN process which produce participating nucleons is illustrated by fig. 1, which represents the distributions of the number of nucleons participating in the  $^{40}\text{Ca} + ^{40}\text{Ca}$  reaction *vs.* impact parameter  $b_{HI}$ , and for different collision energies. As can be seen, the mean-field effects are more important at lower energies, while NN collisions dominate at higher energies. The number of participating nucleons is generally larger for more central collisions. The maxima observed for mean-field nucleons result from an orbiting effect at peripheral collisions. At higher collision energies the mean-field nucleons disappear for central collisions because of competition with the NN interaction.

The distribution of different reaction components in the angular momentum space is presented in fig. 2 ( $^{40}\text{Ca} + ^{40}\text{Ca}$  reaction, 35 AMeV). The cross-section for the creation of a composite system occupies the region of small impact parameters. Cross-sections for events containing at least one IVS cluster with a mass larger than 16, 4, and 1,

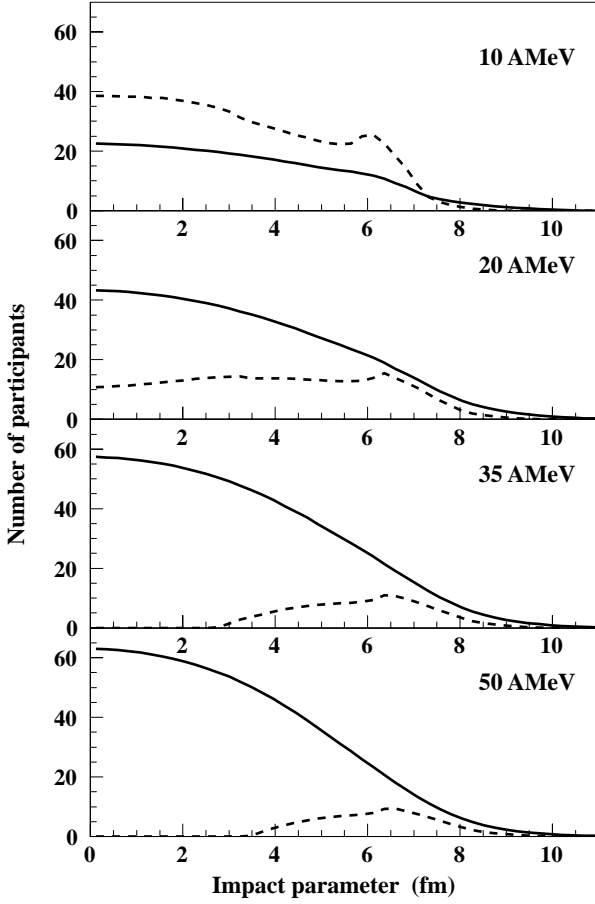


**Fig. 1.** Numbers of nucleons participating in the  $^{40}\text{Ca} + ^{40}\text{Ca}$  reaction *vs.* impact parameter, for different collision energies. NN mechanism (solid line); mean-field mechanism (dashed line).

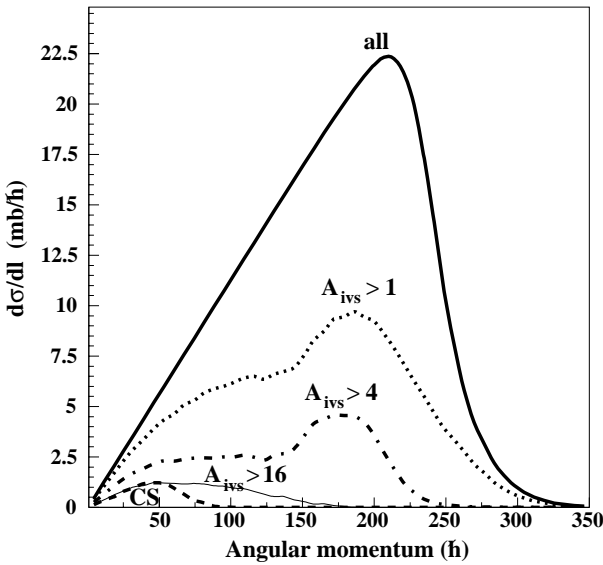


**Fig. 2.** Creation of composite systems, and of IVS clusters with different mass spectra (see text) in different regions of the angular momentum space.

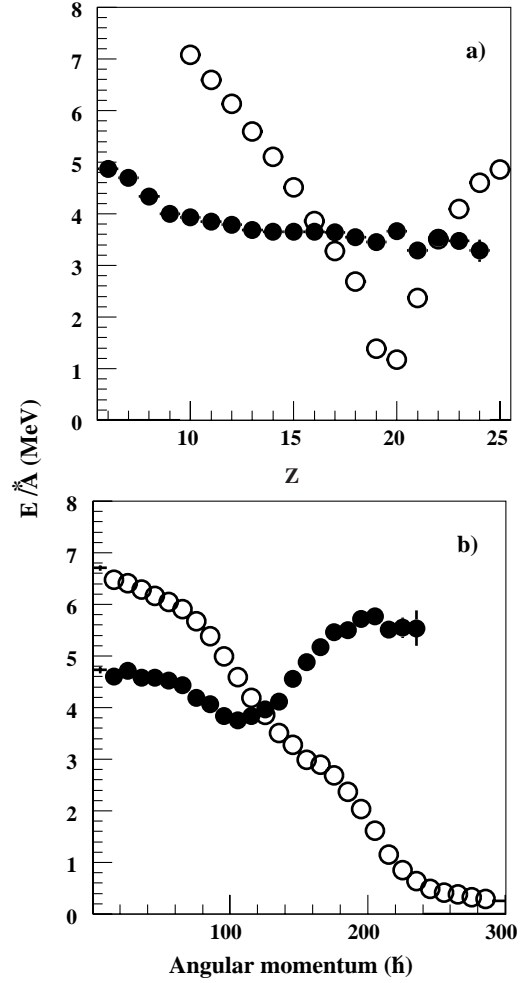


**Fig. 3.** Excitation energy of the IVS (black dots) and of the PLF (or TLF) (open circles) *vs.*  $Z$  (a) or the angular momentum (b).

respectively, are shifted towards higher angular momentum values. It is clear that a deeper penetration of heavy ions and a larger number of participating nucleons is necessary in order to produce heavier clusters (fragments).

Some properties of the intermediate velocity source and of the PLF (or TLF) source produced in the  $^{40}\text{Ca} + ^{40}\text{Ca}$  reaction (35 AMeV) are exhibited in figs. 3 and 4. As can be seen (fig. 3), the average excitation energy per nucleon is almost independent of the IVS size ( $Z$  value). In the case of the PLF (or TLF) it is nearly proportional to the number of caught (or lost) nucleons, showing a minimum at  $Z = 20$ . For the PLF (or TLF) the excitation energy decreases with the angular momentum, and for the IVS increases for more central as well as for peripheral collisions. For more central collisions, there is enough excitation energy for all three sources, due to the large energy dissipation in the entrance reaction channel. For peripheral collisions, the transfer of participating nucleons (or clusters) to the PLF or the TLF is more difficult because of the angular momentum limitations. In consequence, the PLF and the TLF turn into spectators and

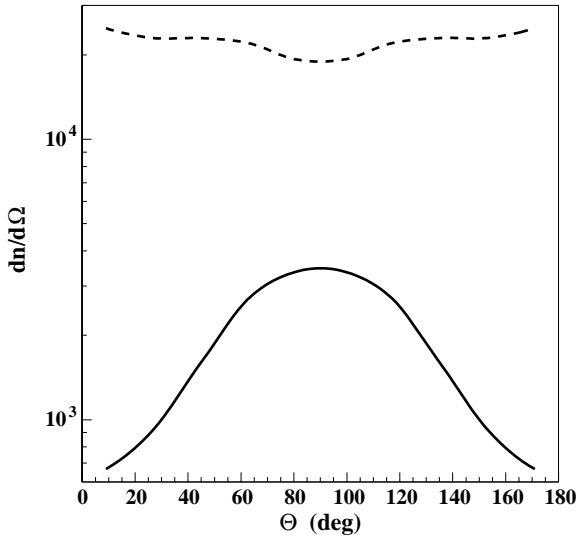


**Fig. 4.** Angular distribution of  $Z > 3$  fragments originating from the IVS, presented in the reference frame oriented by the PLF and TLF (see text). Dashed line: primary IVS fragments; solid line: secondary IVS fragments.

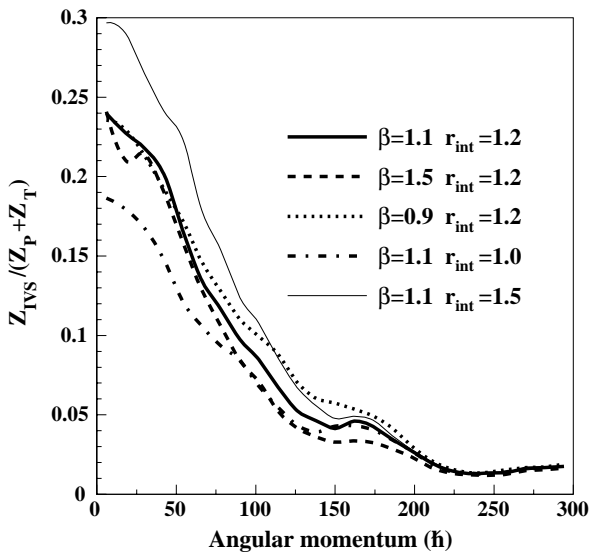


**Fig. 5.** Fraction of the total charge,  $Z_{IVS}/(Z_P + Z_T)$ , vs. angular momentum, for different values of  $\beta$  and  $r_{int}$ .

the IVS absorbs most of the dissipated energy. The number IVS clusters generated at peripheral collisions is small and their contribution to the average excitation energy, for a specific  $Z$  value, is negligible.

The angular distribution of  $Z > 3$  fragments originating from the IVS (fig. 4) is presented in the reference frame oriented by the PLF and TLF. Here,  $\theta$  is an angle between the fragment velocity and the relative PLF-TLF velocity. The distribution of the primary IVS fragments is almost isotropic, while the secondary IVS fragments indicate focusing in the PLF-TLF Coulomb field. The number of the secondary IVS fragments is nearly an order of magnitude lower, because in the evaporation process most of the emitted particles have  $Z < 3$ .

It would be appropriate to ask how sensitive the model predictions are to the values adopted for particular model parameters. Such parameters include, for example: the critical angular momentum  $L_{cr}$  (coefficient  $\beta$ ) or the minimum Coulomb interaction radius ( $r_{int}$ ). Figure 5 shows model predictions for the fraction of the total charge,  $Z_{IVS}/(Z_P + Z_T)$ , located in the intermediate velocity source, and presented vs. angular momentum ( $^{40}\text{Ca} + ^{40}\text{Ca}$  at 35 AMeV). As can be seen, variations of the  $\beta$ , and  $r_{int}$  parameters give noticeable, though not dramatic modifications in the  $Z_{IVS}/(Z_P + Z_T)$  distributions. The model calculations presented in papers I and II [1,2] were performed for  $\beta = 1.1$ , and  $r_{int} = 1.2$  fm.

## 4 Summary and final remarks

We have proposed a model describing heavy-ion collisions, assuming a stochastic reaction mechanism and taking into account the creation of participating nucleons by the mean-field effects as well as the NN interactions. The nucleon transfer probabilities are governed by the state densities, on the average by the maximum value of the thermodynamic probability (entropy). Fluctuations characteristic of the stochastic process are included in the reaction picture.

The modular organization of the PIRAT computer code facilitates its modification. For instance, a simpler (but perhaps less physical) prescription can be used to select the participating nucleon final path along the chain of steps without regard to fluctuations. In this mode, the particular options ( $k, j$ ) taken by a participating nucleon (or cluster)  $k$  are governed by the maximum value of entropy. Similarly, one can assume that for each step  $k$  and option  $j$  along the chain of steps taken by a participating nucleon, the reaction  $Q(k, j)$  energy is divided among the participating subsystems, proportionally to the corresponding densities of states (without including fluctuations). Other prescriptions for the excitation energy ( $Q$  value) partition are also possible, such as that proposed by Wilczynski and Wilschut [23].

Instead of the binary sequential decay of hot fragments, which in the PIRAT code is simulated using the GEMINI [20] or SIMON [21] subroutines, it is also possible to assume a prompt decay picture (for an example, see [24]).

This model contains same numerical parameters having an obvious physical meaning and their values used in our calculations seem to be reasonable.

The predictions produced by this model have been compared with experimental data on the  $^{40}\text{Ca} + ^{40}\text{Ca}$  reaction at 35 AMeV, an energy close to the Fermi energy. Satisfactory agreement and a consistent picture of the reaction mechanism were achieved. Both the properties of the PLF (TLF) source and of the intermediate velocity source were properly reproduced and explained (see [1] and [2]). Comparison with different sets of experimental data is in progress.

Dynamic effects are only partly included in the reaction picture presented here, mainly in the process that se-

lects participating nucleons and in the Coulomb focusing of fragment trajectories. Phenomena related to the compressibility of nuclear matter (nuclear matter equation of state) are not taken into account. This does not seem to pose a great obstacle, however, around the 35 A MeV or at lower collision energy, where such effects are not of prime importance (cf. the systematics of the radial expansion energies [25]).

The author is indebted to K. Grotowski and R. Płaneta for valuable discussions and their assistance in testing the model. The author thanks also A.J. Cole, J. Brzychczyk and A. Wieloch for critical reading of the manuscript. This work was supported by the Scientific Research Commission of Poland (KBN Grant PB 1188/P03/98/14) and the M. Skłodowska-Curie Fund (MEN/DOE- 97-318). Calculations for this work were partly performed using facilities of the Cracow Academic Computing Center, CYFRONET (KBN Grant No. S2000/UJ/158/1998).

## References

1. R. Płaneta et al., this issue, p. 297.
2. Z. Sosin et al., this issue, p. 305.
3. J. Aichelin, G. Bertsch, Phys. Rev. C **31**, 1730 (1985).
4. H. Kruse et al., Phys. Rev. C **31**, 1770 (1985).
5. J.F. Dempsey et al., Phys. Rev. C **54**, 1710 (1996).
6. C. Gregoire et al., Nucl. Phys. A **465**, 317 (1987).
7. J. Aichelin, H. Stoecker, Phys. Lett. B **176**, 14 (1986).
8. T. Neff, H. Feldmeier, R. Roth, J. Schnack, *Proceedings of the 27th International Workshop on Gross Properties of Nuclei and Nuclear Excitations-Multifragmentation, Hirschegg, Austria*, edited by H. Feldmeier, J. Knoll, W. Norenberg, J. Wambach, (Darmstadt, GSI, 1999) p. 283.
9. A. Uno, H. Horiuchi, Phys. Rev. C **53**, 2958 (1996).
10. B.G. Harvey, Nucl. Phys. A **444**, 498 (1985).
11. A.J. Cole, Z. Phys. A **322**, 315 (1985); A.J. Cole, Phys. Rev. C **35**, 117 (1987).
12. L. Tassan-Got, C. Stéphan, Nucl. Phys. A **524**, 121 (1991).
13. D. Durand, Nucl. Phys. A **541**, 266 (1992).
14. Z. Sosin, K. Grotowski, A. Wieloch, H.W. Wilschut, Acta Phys. Polonica, B **25**, 1601 (1994); Z. Sosin et al., Nucl. Phys. A **574**, 474 (1994).
15. J. Randrup, Nucl. Phys. A **307**, 319 (1978).
16. P.J. Karol, Phys. Rev. C **11**, 1203 (1975).
17. D.H.E. Gross, Rep. Prog. Phys. **53**, 605 (1990).
18. P. Bonche, S. Levit, D. Vautherin, Nucl. Phys. A **427**, 278 (1984).
19. Bondorf et al., Phys. Rep. **257**, 133 (1995).
20. R.J. Charity et al., Nucl. Phys. A **483**, 371 (1988).
21. D. Durand, unpublished.
22. W. Gawlikowicz, Acta Phys. Polonica B **28**, 1687 (1997).
23. J. Wilczynski, H.W. Wilschut, Phys. Rev. C **14**, 2475 (1989).
24. W. Gawlikowicz, K. Grotowski, Nucl. Phys. A **551**, 73 (1993).
25. B. Borderie, preprint IPNO-DRE-96-22; R. Pak et al., Phys. Rev. C **54**, 1681 (1996); W.C. Hsi et al., Phys. Rev. Lett. **73**, 3367 (1994); H.W. Barz et al., Nucl. Phys. A **531**, 453 (1991); S.C. Jeong et al., Phys. Rev. Lett. **72**, 3468 (1994); M.A. Lisa et al., Phys. Rev. Lett. **75**, 2662 (1995).